



Hydrogen Production *via* Cracking of Methane at Low Temperature- A Review Paper

Atideepth Bharadwaj*, Arshad Arif CM, Surya Kant

Abstract

This paper reviews the development of catalysts to produce hydrogen and carbon by cracking methane into its components. Multiple catalysts that have been viewed and studied will be reviewed. The effectiveness of the catalyst will depend upon the conversion rate, rate of deactivation and even the purpose of use of the hydrogen and carbon formed. In the papers reviewed, each catalyst was analysed by various methods like (XRD, SEM, TGA, Raman Spectroscopy, etc.). A few alternative methods to produce hydrogen, those which can be used in different situations depending on the use of the by-products, will be listed as well. The conversion rates, analysis results and drawbacks of each method/catalyst are compared along with other essential data being presented as well. The final selection contains more than one catalyst as it depends on the purpose of the products and the circumstances in which the hydrogen is being produced or will be used.

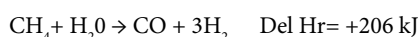
Keywords

Hydrogen Production; Methane Degradation; Catalyst; Carbon Nanotubes

Introduction

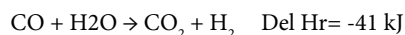
In the current day and age, global warming and pollution are one of the major problematic phenomena that cause instability and harm to the environment. The necessity to reduce greenhouse gases that are the major cause of these phenomena has never been more. Excessive usage of fossil fuels, which has caused environmental concern, has stimulated exploration into the development of alternative renewable energy sources. More and more methods are being devised to reduce the carbon footprint of the world by moving towards more "clean" fuels like renewable sources (wind, solar, hydro, etc.) and particularly Hydrogen [1].

Hydrogen has massive potential as a fuel due to the large amount of energy it stores in its atoms and does not release any greenhouse gases like Carbon Dioxide. The production of Hydrogen has been traditional from hydrocarbons like methane which when they undergo Steam Reforming (SRM), which is the reaction with water at a high temperature to produce hydrogen [2].

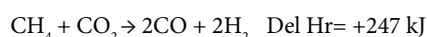


*Corresponding author: Atideepth Bharadwaj, Department of Chemical Engineering, National Institute of Technology, Surathkal, Karnataka, India, Telephone: +91 8861192803; E-mail: atideepth@gmail.com

Received: July 30, 2021 Accepted: August 27, 2021 Published: September 21, 2021

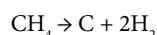


The other methods include dry reforming of methane, which is reaction of methane with Carbon Dioxide [2].



The advantage of DRM over SRM is that it can directly use the Carbon Dioxide in the atmosphere or use the emissions from other industries as its raw material, which helps reduce its release into the atmosphere.

However, in both these methods, there is some form of either CO_2 or CO that is being emitted. Therefore, a better method would be to completely split this Methane gas into its constituent elements i.e. Carbon and Hydrogen. If we use a suitable catalyst then this method would be called Catalytic Decomposition of Methane (CDM).



This reaction takes place at a variety of temperatures ranging from a few hundred degrees Celsius to a few thousand. Depending on the use of different catalysts and promoters, we get various conversion rates of methane at different temperatures. The goal of this review paper is to try to find the most suitable method to produce Hydrogen at the lowest temperature with the highest possible conversion rate.

Different kinds of literature were reviewed in order to see how different catalysts reacted at different temperatures using different methods. The most common catalysts used were Iron, Nickel among others [2-18]. These were doped with different compounds and the experiments were conducted using different methods.

There were many similarities among the various findings in each of the methods. The most common difficulty was that the catalyst deactivated after a certain period as the carbon produced in the reaction clogged the pores of the catalyst thus reducing its activity. The other one was that most of the reactions took place above 700 degree Celsius [2-18]. But there were few that had a positive response at lower temperatures as well [7,9,11,13-15]. There were ways to tackle this problem, as it was possible to make this carbon react with steam parallelly. This reaction will give hydrogen and carbon monoxide. This will produce more hydrogen than the original and prevent the catalyst from deactivating. The carbon monoxide produced can also be further used in the water gas shift reaction ultimately giving more hydrogen.

Materials and Methods

Catalysts

There are multiple catalysts that can be used with different combinations of promoters and supports in order to help them work better. We will be mentioning the list of some of the catalysts we have reviewed and their working along with the experimental procedures.

As stated before the main catalysts used in most of the cases were either Iron or Nickel along with a couple of rare cases using cobalt and platinum as well.

The preparation of most catalysts uses wet impregnation, which allows the active metal precursor to be dissolved in an aqueous or

organic solution. Then the metal-containing solution is added to a catalyst support containing the same pore volume as the volume of the solution that was added. Capillary action draws the solution into the pores. Solution added in excess of the support pore volume causes the solution transport to change from a capillary action process to a diffusion process, which is much slower. The catalyst can then be dried and calcined to drive off the volatile components within the solution, depositing the metal on the catalyst surface [19].

The most studied catalysts for the CDM are Nickel supported on: SiO_2 , TiO_2 , graphite, ZrO_2 , $\text{SiO}_2\text{-Al}_2\text{O}_3$, Al_2O_3 [2,3,5,12,17], MgOSiO_2 , MgO and ZnAl_2O_4 among others [11]. Iron-based catalysts perform better at higher operating temperatures than Ni catalysts for the CDM process. Thus, it is possible to obtain higher CH_4 conversions with Fe catalysts than with Ni catalysts since they can be used above 700°C , resulting in a positive shift in the equilibrium [3]. However, as we wanted to focus on achieving conversion at lower temperatures, this wasn't a viable option.

Spray-dried $\text{Fe}_2\text{O}_3/\text{Al}_2\text{O}_3$ is an effective carbon carrier for catalytic methane cracking. Spherical, porous and fluidizable catalyst has been produced by spray-drying of 10 wt% Fe_2O_3 and 90 wt% Al_2O_3 . This material can accommodate the deposited solid carbon from the methane cracking reaction in its pores [2]. The advantage of this approach is that CO_2 is used as a reactant that could be obtained by capture from industrial point sources or directly from air. In this way, it can then be used as a carbon source in chemical synthesis and thus replace fossil fuels. In catalysts, first-row transition metals offer the advantage of lower cost over Pt-group metals and higher reactivity than carbon-based catalysts [20].

However, some transition metals may get oxidized by CO_2 in the regeneration step as an undesired side reaction [2]. Ni is burdened by high cost and toxicity issues, considering Fe-based (cheap and environmentally benign) catalysts. The catalyst is in the form of fluidizable particles and is circulated between the beds. This design of such fluidized catalyst particles is crucial. Al_2O_3 was chosen as a support material due to the high cracking reactivity of $\text{Fe}/\text{Al}_2\text{O}_3$ materials. The bed material used in all experiments was spray-dried $\text{Fe}_2\text{O}_3/\text{Al}_2\text{O}_3$ [2].

Fe and Fe-Ni supported catalysts were used in methane decomposition. The support doped with La_2O_3 gave the best performance in terms of CH_4 conversion, H_2 yield, and stability at the test conditions, 800°C and $4,000 \text{ mlh}^{-1}\text{g}^{-1} \text{ cat}/\text{Space velocity}$. The addition of Ni significantly improved the performance of all the monometallic catalysts. The La_2O_3 promoted support gave the best performance and maintained good stability during the time on stream [4].

The effects of different supports such as La_2O_3 , ZrO_2 , SiO_2 , Al_2O_3 , $\text{SiO}_2/\text{Al}_2\text{O}_3$, and TiO_2 on Ni-based catalysts have been studied. Ni catalysts are effective for methane decomposition reaction at temperatures of 500°C - 600°C , which are below the equilibrium-required temperature. At higher temperatures, Ni catalysts deactivate rapidly, but Fe can withstand these necessary high temperatures. As mentioned before, Fe is relatively cheaper than Ni. Monometallic Fe and bimetallic Fe/Ni-based catalysts supported over zirconia and modified zirconia were used for the catalytic decomposition of CH_4 [4]. An advantage of the gauze form of Nickel catalyst is the possibility to arrange a structured catalytic bed, characterized by a low-pressure drop during the passage of gases through the reactor [9].

The introduction of rare earth elements into $\text{Ni}/\text{Al}_2\text{O}_3$ led to the formation of a hydrotalcite-like structure, which greatly changed the activity of Ni particles. Among them, the $\text{Ni}/\text{Re}/\text{Al}_2\text{O}_3$ catalysts present the best methane conversion due to the large surface area of Ni particles and the strong interaction between Ni and $\text{Re}/\text{Al}_2\text{O}_3$ [21,22].

Carbon can form catalytically on Ni surfaces and the carbon formation is more likely to be related to kinetic rather than to thermodynamic considerations. One solution for avoiding carbon deposition problems associated with Ni-based anodes, is to replace Ni with Cu [23,24], which is not a catalyst for carbon formation. However, Cu is not a good oxidation catalyst and has a relatively low melting temperature, which decreases the anode stability. Further, the low melting temperature of copper oxides makes the fabrication procedures typically used for Ni-cermetts impossible. The second strategy is to use ceramic materials, which do not catalyze carbon formation. Among these materials, highly conductive perovskites have received much attention for direct hydrocarbon conversion in SOFCs [10].

In certain cases, carbon is produced as a by-product in the form of carbon nanofibers, carbon nanotubes, multiwall carbon nanotubes, bi wall nanotubes and fish-bone type carbon depending upon the operating conditions [25]. This carbon has excellent surface properties, high mechanical strength, highly resistant to acids and bases, high surface area, highly electronegative. It can also be used as catalyst and catalyst support, adsorbent, conductive polymer and as composite material [12,26,27].

One of the rarer catalysts used was a combination of $\text{CoO-MoO}/\text{Al}_2\text{O}_3$. However, the goal was to obtain Carbon Nano tubes rather than hydrogen production. CoO-MoO metal loadings were used in an increasing manner. An increasing in the metal loading increased the carbon yield and broadened the diameter distribution of the as-produced Carbon nanotubes, but too much of an increase of metal loading retarded the carbon yield. The highest carbon yield was recorded for the catalyst with 30 wt% metal loading. Here, the catalytic activity can be related to the cobalt oxide crystallite size [17].

Metals that are active catalysts for methane (Ni, Pt, Pd), when dissolved in inactive low melting temperature metals (In, Ga, Sn, Pb), produce stable molten metal alloy catalysts for pyrolysis of methane into hydrogen and carbon. All solid catalysts previously used for this reaction have been deactivated by carbon deposition. In the molten alloy system, the insoluble carbon floats to the surface where it can be skimmed off [18].

Finally one method that we found intriguing was the transformation of methane and carbon dioxide into synthesis gas was performed by plasma discharge coupled with a catalyst. The synergy between plasma and catalyst is then clearly demonstrated at 300°C whereas at room temperature the effect remains very low. The catalyst surface modification under the plasma discharge was evidenced by Raman spectroscopy, a strong fluorescence effect being visible after reaction under plasma at 300°C . As an alternative to conventional catalytic DRM reaction, non-thermal plasma appears as an interesting technology since highly energetic electrons generated by plasma are able to initiate the chemical processes at room temperature [7].

Methods

- **X-Ray Diffraction (XRD):** X-Ray Diffraction is a technique for characterizing crystalline materials. It provides information

on structures, phases, preferred crystal orientations, and other structural parameters (average grain size, crystallinity, strain, and crystal defects). This is done by irradiating a material with incident X-rays and then measuring the intensities and scattering angles of the X-rays that leave the material. [2-5,11,13-15]

- **Scanning Electron Microscopy (SEM):** This technique is used to get a higher resolution image of a specimen in three-dimensional. It works on the principle of scattering electrons on the surface. The electrons which get reflected from the sample after the bombardment are collected to get the image of the specimen. The SEM images are used for various research studies and applications [2-5,8-10,12-15].

- **Thermo-Gravimetric Analysis (TGA):** Thermogravimetry is the technique in which the change in weight is recorded as the function of temperature or time. This method is used to determine a material's thermal stability. But only solid substances can be analysed by this method [4,5,12,13].

- **Transmission Electron Microscopy (TEM):** Transmission electron microscopy is the technique in which a beam of electrons is transmitted through a specimen to form an image. An image formed from the interactions of the electrons with the samples as the beam is transmitted through the specimen. Through this analysis we can get information about the surface features, shape, size and structure of the specimen [2-6,8,11,15].

- **Thermal conductivity:** Thermal conductivity is a measure of the rate of transfer of energy. The coefficient of thermal conductivity is defined as the rate of transfer of energy across unit surface area when there is a unit temperature gradient perpendicular to the surface. Materials with high thermal conductivity are good for conducting thermal energy. Therefore, materials of high thermal conductivity are widely used in heat sink applications, and materials of low thermal conductivity are used as thermal insulation [12].

- **Laser Diffraction Particle Size Distribution Analyser:** Laser diffraction particle size analyzers are used to measure the size of particles in a material. Particle size is calculated by measuring the angle of light scattered by the particles as they pass through a laser beam. Particle distribution is important for understanding the physical and chemical properties of a material. This technique has emerged as one of the most important and effective methods for particle size analysis which is fast, non-destructive, suitable for a broad range of particle sizes [2].

- **Raman Spectroscopy:** Raman Spectroscopy is a chemical analysis technique that provides information about chemical structure, phase and polymorphy, crystallinity and molecular interactions. In this technique, scattered light is used to measure the vibrational energy modes of a sample. This technique can differentiate chemical structures, analyse samples multiple times without damage, also used in chemistry to provide a structural fingerprint by which molecules can be identified. One of the real-life applications is used to detect explosives from a safe distance using laser beams [7,4,14].

- **Infrared Spectroscopy (IR Spectroscopy):** This is a technique that deals with the infrared region of the electromagnetic spectrum, that is light with a longer wavelength and lower frequency than visible light. It covers a range of techniques, mostly based on absorption spectroscopy. Just like all spectroscopic techniques, it can be used to identify and study chemicals. A common laboratory instrument

that uses this technique is a Fourier transform infrared (FTIR) spectrometer [7].

- **Brunauer-Emmett-Teller Analysis (BET):** This technique explains the physical adsorption of gas molecules on a surface and can be used for the measurement of the specific surface area of materials. Nitrogen is the most commonly employed gaseous adsorbate used for surface probing by this method. One of the implementations of this technique is to estimate the specific surface area of activated carbon from experimental data [4,5,14,15].

- **Temperature-Programmed Reduction/Oxidation (TPR/TPO):** This is a material characterisation technique commonly used in catalysis studies to examine the surface chemistry of metals and metal oxide under different thermal conditions. TPR is an integral part of catalyst investigation, as we get accurate data regarding catalyst reducibility and reaction rates in the presence of metal surfaces. TPO is a popular application in the research and development of alternative energy fuels and increased energy efficiency in chemical manufacture [4,14,13].

Results

In the case of using spray-dried $\text{Fe}_2\text{O}_3/\text{Al}_2\text{O}_3$ the reduction with H_2 was found to be practically infeasible due to unfavourable kinetics [2]. Instead, a reduction in a stronger reducing gas such as CH_4 is likely required for practical application. In the Methane cracking using $\text{Fe}_2\text{O}_3/\text{Al}_2\text{O}_3$ catalyst, it is clear that the CH_4 cracking reaction to form solid carbon and produce H_2 is initially very fast and then subsequently slows down as more carbon is deposited on the material. Deactivation of the bed material for the methane cracking reaction was observed and found to be independent of reaction temperature. The deactivation could be well described by assuming a linear decline in cracking activity with the amount of carbon deposited on the material. Analysis of the spent bed material revealed that up to 10 wt% of carbon could be deposited on the material without affecting the integrity and fluidization properties of the spray-dried particles. More than 10 wt% carbon deposition led to loss of mechanical integrity of the particles and accompanying bed volume increase, independent of the reaction conditions [2].

In the case of $\text{Fe}_2\text{O}_3/\text{Al}_2\text{O}_3$ used in a fluidised bed reactor the catalyst allows for hydrogen production and high quantities of carbon nanofilaments with interesting structural and textural properties [3]. Carbon is deposited mainly as nanofilaments emerging from the catalyst particles. As a result, the density and shape of the particles in the reactor, and thus their fluid dynamical behaviour, dramatically change as the carbon monofilaments grow. The operating conditions play an important role in the performance of the catalyst. At a low reaction temperature of 700°C , low methane conversions of 15% were observed, the catalyst deactivation was slow, although there was a long induction period of two hours that was not present at higher temperatures. The best catalyst performance was obtained at 800°C , where the average carbon deposition rate was higher. Space velocity also has a principal role in the methane decomposition reaction through its effect on the gas-solid contact. The decrease in Space velocity showed a significant increase in conversion rate. An increase in the temperature or a decrease in the weighted hourly space velocity increases the methane conversion but also accelerates the deactivation of the catalyst. At a reaction temperature of 800°C and space velocities in the range of 3-8 $\text{LN}/(\text{gcat h})$, high hydrogen production with relatively low catalyst deactivation is observed. Under these

operating conditions, carbon is deposited as long nanofilaments, mainly multiwall carbon nanotubes, and the Fe based catalysts show a relatively low decay deactivation pattern [3].

When we look at Fe-Ni supported catalysts [4], the relative intensities of all the diffraction peaks of Fe supported on the $\text{La}_2\text{O}_3+\text{ZrO}_2$ catalyst were more pronounced compared with those of the other catalysts. This indicates that the introduction of La_2O_3 in the catalyst structure improved the dispersion of the metal particles. The addition of Ni led to an increase in the surface area of the catalysts, except for 20%Fe+20%Ni/ ZrO_2 . This could be due to the doping effect and the aggregation of the metal particles due to the weak metal-support interaction. 40%Fe/ $\text{La}_2\text{O}_3+\text{ZrO}_2$ has the least hydrogen uptake from among the single metal-supported catalysts, which implies that it could be activated with ease at moderate temperatures [4].

Same trend of reduction was observed for the bimetallic catalyst samples. The observed difference is that peaks of higher intensity/ H_2 consumption were observed for the bimetallic samples owing to the presence of an additional metal oxide, i.e. NiO. Moreover, the reduction peak of NiO at a temperature of $\sim 350^\circ\text{C}$ for the Fe-Ni/ ZrO_2 catalyst disappeared after incorporating La_2O_3 and WO_3 in the catalyst compositions. These dopants enhance the metal dispersion. The reduction peaks for the bimetallic samples appeared at lower temperatures relative to the single metal supported samples. For bimetallic catalysts, the addition of Ni increased the activity of the catalysts, with the most active catalyst having the highest amount of carbon deposits [4]. The addition of Ni promoted the formation of filamentous-graphitic carbon whose growth does not hinder access to the active metal sites. The formation and growth of filamentous carbons during catalytic methane decomposition was beneficial in keeping the active Ni sites accessible for CH_4 molecules and, consequently, made it possible for the catalysts to maintain their activity and stability for a longer time [28]. (Figures 1 and 2)

In the case of Ni/ Al_2O_3 with either Pd or Cu, the effect of promoting 50% Ni/ Al_2O_3 with Cu (15%) and Pd (0.9%) is evident from diagram that the catalytic activity and the stability have improved adding Cu and Pd on parent catalyst [29]. The presence of Cu enhances the catalytic efficiency as it has been proposed that graphene has a larger affinity with Cu, which inhibits its encapsulation on the surface of Ni. Moreover, the dispersal of coke in Pd is cited to be six times faster than Fe, Ni or Co [5,30]. The coke produced on 50%Ni-15%Cu-0.9% Pd/ Al_2O_3 as carbon nanofibers. Relatively wider carbon nanofibers are seen deposited on 50% Ni-15% Cu-0.9% Pd/ Al_2O_3 as compared to 50% Ni/ Al_2O_3 . The Field Emission SEM analysis also discovered that the basic appearances of Carbon nanofibers were influenced by the adding of Cu and Pd promoters on Ni/ Al_2O_3 . Cu and Pd have the tendency to promote the dispersion of Ni on alumina and increase the dispersion rate of carbon which facilitates the catalyst performance [5] (Figure 3).

If we consider Ni with $\text{TiO}_2/\text{SiO}_2/\text{Al}_2\text{O}_3/\text{MgO}$, the methane decomposition obtained within the first 5 min of reaction decreased in the order $\text{SiO}_2 > \text{Al}_2\text{O}_3 > \text{TiO}_2 > \text{MgO}$ support. After 60 min on stream, the order of activity changed to $\text{TiO}_2 > \text{SiO}_2 > \text{MgO}$ support, and a pressure build-up (PB) was observed on the Al_2O_3 support. At 120 min on stream, the TiO_2 system maintained its activity, and the MgO decreased, whereas a pressure buildup occurred in the SiO_2 -supported catalyst system. The TEM image of the carbon formed using Ni on the TiO_2 support was the best among the supported catalysts [6] (Figure 4).

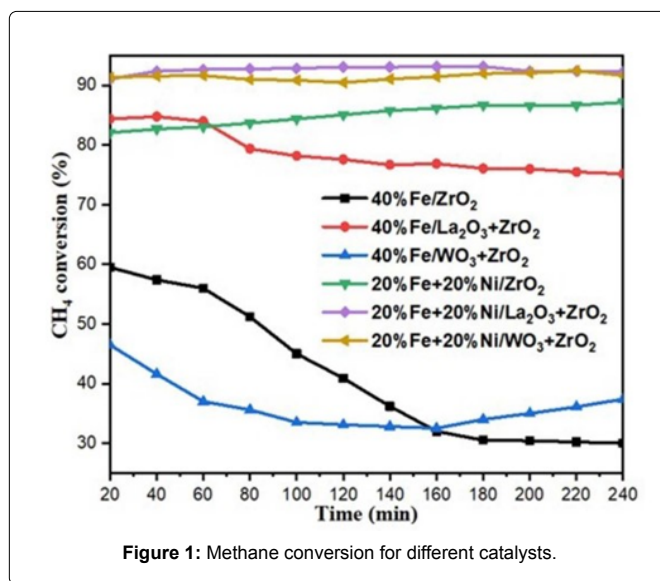


Figure 1: Methane conversion for different catalysts.

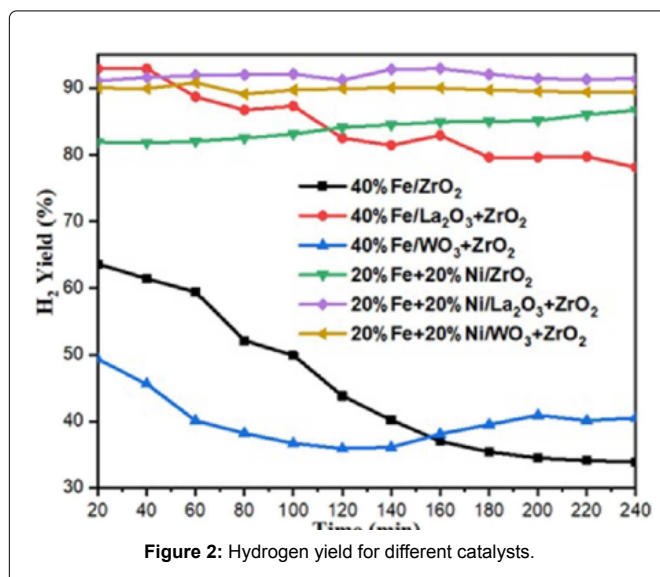


Figure 2: Hydrogen yield for different catalysts.

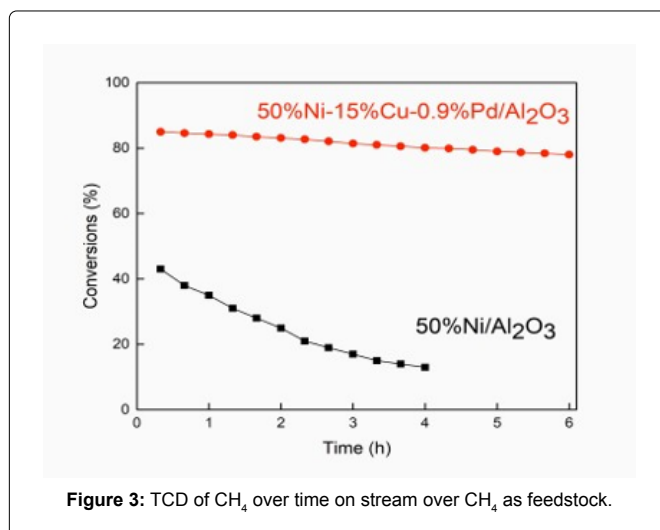


Figure 3: TCD of CH_4 over time on stream over CH_4 as feedstock.

In a specific case for Ni/SiO₂, the formation of carbon filaments as a result of hydrocarbon cracking was reported with higher molecular weight hydrocarbons over supported Nickel, iron, cobalt and several alloy catalysts [31-39]. Carbon filament formation at low temperatures is expected to be hindered by the low solubility of carbon in Nickel, while at high temperatures methane cracking is much faster than the bulk diffusion and surface migration. In both cases, the Nickel surface quickly becomes fully covered with carbon, leading to the interruption of the catalytic cycle [8,40].

These catalysts maintain their activity for a sustained period of time because of their capability to accumulate large amounts of carbon on their surface in the form of long cylindrical hollow filaments, with a Nickel particle located at the front tip of each individual filament. Deactivation eventually occurs due to spatial limitations imposed on the filament growth, which leads to the loss of exposed Nickel surface. The deactivated catalyst can be fully regenerated by either oxidation in air or steam gasification of the deposited carbon. Additional hydrogen is produced during the steam regeneration process [8] (Figure 5).

The Ni-grid with Raney-type outer layer was shown to be active for this reaction at relatively low temperatures of 450°C-500°C. Deactivation of the catalyst occurs through the coke deposition in the form of filamentous carbon as shown by SEM. The deactivated catalyst can be regenerated in the oxidative atmosphere. Therefore, the direct catalytic cracking was followed by catalyst regeneration during periodic reactor operation. The temperature strongly affects the conversion and the selectivity of the process towards hydrogen and carbon oxides formation [9].

When we use Ceria coated Nickel in a Solid Oxide Fuel Cell (SOFC) in order to produce hydrogen, surface-seated Nickel is believed to be a good catalyst for fuel oxidation at the anode. However, when CH₄ is used as fuel, Nickel is also a good catalyst for carbon deposition, which should be avoided in SOFCs. Although pre-reforming is an effective way to overcome this problem, in-situ reforming and direct electrochemical oxidation at the anode is always a hot topic in SOFC research [41,42]. One possible way to avoid carbon deposition is to cover Ni particles with materials inert to carbon formation [10].

An anode-supported SOFC with a modified Nickel-cermet anode running directly for methane exhibits good cell performance and long-term stability without carbon deposition. Nano sized Sm Doped Ceria (SDC) particles were coated uniformly onto the Nickel particles of the anode using an ion impregnation method. When both humidified hydrogen and methane were used as fuel, the anode area-

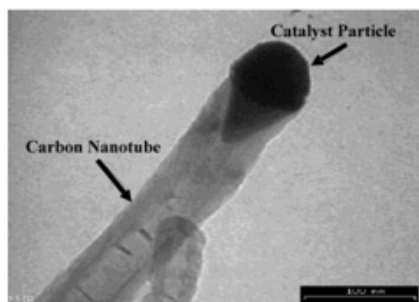


Figure 4: Transmission electron microscope image of carbon formation on the catalyst particle.

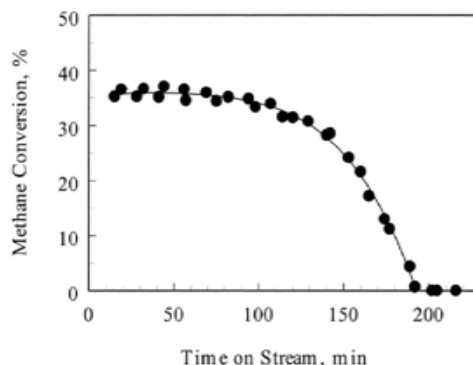


Figure 5: Deactivation of the Ni/SiO₂ catalyst at 823 K and GHSV=30 000 hy⁻¹ (feed: 20% CH₄, balance He).

specific resistance decreased and cell performance increased with the SDC loading on the anode through this impregnation, inferring that the SDC coating on the Nickel surface could effectively increase the number of triple-phase boundaries [10].

Another experiment that also used Cerium doped Nickel used different methods for their experiment. The distribution of the NiO particles on the surface of the various supports is different. It has been proved that CeO₂ may enhance the metal dispersion on it due to the interaction between CeO₂ and the metal center [43,44]. In their catalysts, the surface of CeO₂, NiO oxide was uniformly distributed with high dispersion. In the cases of SiO₂-CeO₂ as support, silica addition lowers the interaction of the support and the metal oxide, which might lead to low dispersion of the NiO oxide. SiO₂ and SiO₂-nCeO₂ were effective supports of Ni for the catalytic decomposition of methane into hydrogen and carbon [11].

The amount of loading on the catalyst plays an important role in the conversion rates. In the case of a study of Nickel loadings on Ni/Al₂O₃, the highest methane conversion is given by 50wt% Ni/Al₂O₃ as shown in the figure. Methane conversion increases with the rise in temperature due to the endothermic nature of the reaction. The same trend was observed for 50wt% Ni/Al₂O₃ as methane conversion increased at higher temperatures. The deactivation time of the catalyst was decreased as the reaction was very fast and Ni became inactive to diffuse carbon in it. The other figure shows methane conversions at different temperatures. However, Better results were obtained by using methane methanol mixture as methanol decomposes at lower temperatures and gives much reactive carbon as compared to methane. Thus it adds stability and reactivity to thermocatalytic decomposition of methane [12] (Figures 6 and 7).

For the production of CO/CO₂-free hydrogen and nano-structured carbon over iron-based catalysts supported on magnesia and titania [13]. The catalysts with different loadings of Fe were prepared and tested in a micro activity fixed bed reactor. The activity results revealed that Fe based catalysts supported on magnesia presented better performance as compared to titania supported catalysts. Among the Fe-Mg catalyst series, 30 Fe-Mg remained the best catalyst among the series. Hydrogen reduction temperature of 500°C was found pertinent for catalyst activation. A maximum hydrogen yield of 46.7% and carbon yield as high as 5.5 gC/gFe were

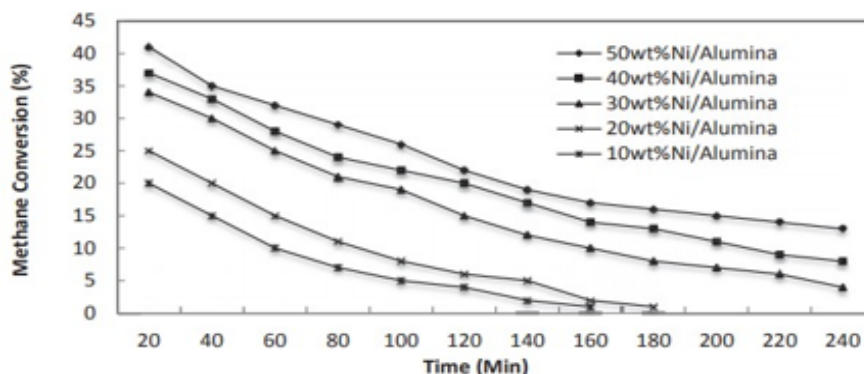


Figure 6: Effect of Ni loading on methane conversions, Reaction Conditions: 550OC, GHSV: 18,000 ml/hr.gca.

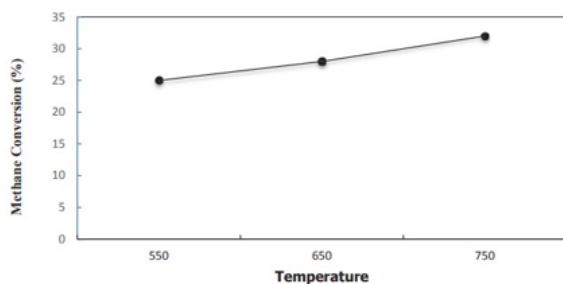


Figure 7: Effect of reaction temperatures on methane conversions, Ni loadings: 50wt%Ni/Al₂O₃, GHSV: 18,000 ml/hr.gca.

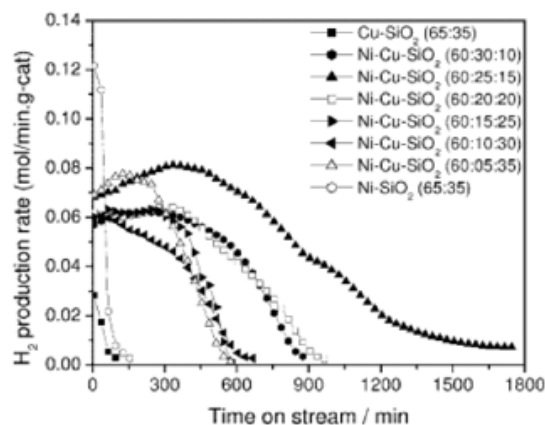


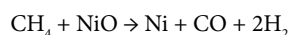
Figure 8: Hydrogen production rates as a function of time on stream over Ni-Cu-SiO₂ catalysts during methane decomposition at 650°C.

obtained over 30 Fe-Mg catalysts. Morphological analysis of spent 30 Fe-Mg catalysts revealed the formation of carbon nanofibers [13].

For a combination of Ni-Cu-SiO₂ methane decomposition activities were carried out over Ni-Cu-SiO₂ catalysts having constant Ni amount and varied Cu/Si ratios at 650°C and atmospheric pressure [14]. Decomposition results revealed that the quantity of Cu present in Ni-Cu-SiO₂ catalysts significantly influenced methane decomposition activity of Ni. The decrease in the catalyst activity is due to a higher amount of copper, which may make the catalyst particles easily become quasi-liquid and which may weaken their stability at high temperatures. Moreover, the presence of Cu in Ni-SiO₂ systems significantly enhances its catalytic performance besides the poor catalytic performances of Ni-SiO₂ and Cu-SiO₂ systems alone. However, it has been proposed that copper has a high affinity with the graphite structure, which inhibits the formation of a graphite layer on the Nickel surface. This effect of copper may reduce the growth rate of carbon layers on the Nickel surface and, therefore, the encapsulation of catalyst particles by carbon layers is retarded, which is regarded as the main reason for the catalyst deactivation [14] (Figure 8).

Nickel and five different supported molten metal catalysts comprising varying quantities of Nickel and lithium supported on calcium oxide were synthesized and designated according to weight % as; 50% Ni/CaO, 37.5% Ni- 12.5% Li/CaO, 25.0% Ni- 25.0% Li/CaO,

12.5% Ni 37.5% Li/CaO, and 50% Li/CaO [15]. Methane reacted with NiO to give H₂, CO₂, and metallic Nickel as per the equation:



Part of the produced hydrogen was also used in the Nickel oxide to metallic Nickel reduction process, hence low hydrogen yields. The presence of surface oxygen completed further oxidation of the process CO into CO₂. The catalyst became more stable at higher temperatures due to expulsion of residual moisture and availability of active Nickel sites which became evenly distributed in the molten lithium hydroxide until 650 °C. Nickel catalyst is usually active within a narrow range of temperature 623 K to 823 K within which a maximum conversion level of 60% can be achieved. At temperatures higher than 923 K, Nickel loses its stability because the coke formed in the reaction tends to grow on the metal (encapsulating carbon) which drastically reduces the active sites of the catalyst [15].

Hydrogen yields started to decline after 650°C because of coke deposition on the molten catalyst and near decomposition temperature of lithium hydroxide, which is at 780°C. At that

point, the catalyst ceased to function as a supported molten metal catalyst [15]. Individual Nickel metal particles are believed to have facilitated the diffusion of methane molecules to the catalyst surface and thus favouring the growth of Carbon Nanotubes (CNT) [45]. Catalyst 50% Ni/CaO showed 60.2% methane conversion and 35.7% hydrogen yield in CDM reaction. Modification of catalyst 50% Ni/CaO by introduction of lithium hydroxide improved its performance greatly. Activity results of 37.5% Ni-12.5% Li/CaO catalyst displayed outstanding results among all the catalysts by having 65.7% methane conversion and 38.3% hydrogen yield at 650 °C [15] (Figures 9 and 10).

A series of Pt-promoted Nickel-Ceria catalysts were used for methane decomposition. Rather than using commercial Ceria, urea-assisted solid-state combustion derived porous Ceria was used as a catalyst support. Various characterization results indicated an enhanced role of the Pt and Ceria support towards the catalytic activity

of the catalysts. The active phase of Nickel was found to be NiO, which was highly dispersed on the surface of the ceria. The addition of platinum as a promoter increased the metal oxide surface dispersion rate. The specific surface area of the Ni/CeO₂ catalyst increased with the addition of Pt, and with increasing amounts of Pt, the surface area of the Pt promoted catalyst also increased considerably. This could be attributed to the synergistic effects of Pt and Ni over Ceria [46]. Moreover, the reduction temperatures were found to be lowered after Pt addition due to the hydrogen spillover effect [47]. The scanning and transmission electron microscopic images indicated the presence of a porous network in the catalysts produced by the inter-aggregation of particles [16].

Among the synthesized catalysts, the 0.2% Pt Ni/CeO₂ catalyst showed the highest hydrogen yield. A maximum hydrogen yield of 65% was observed for the catalyst at 750°C. No catalyst deactivation or formation of CO_x was detected, which might have been due to the

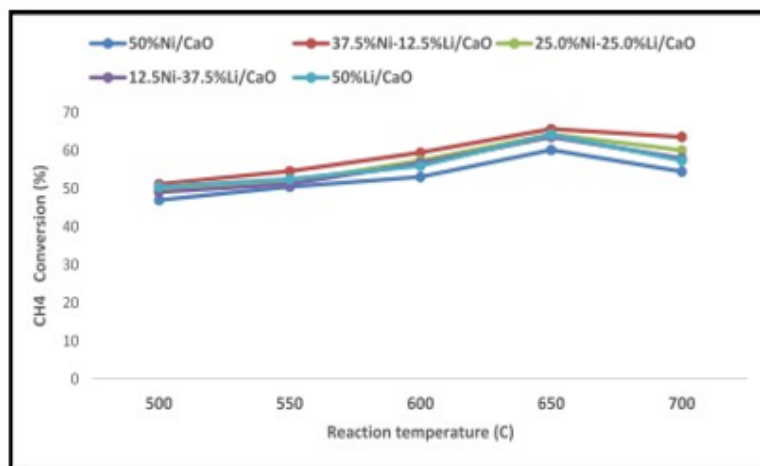


Figure 9: Effect of reaction temperature on methane conversion.

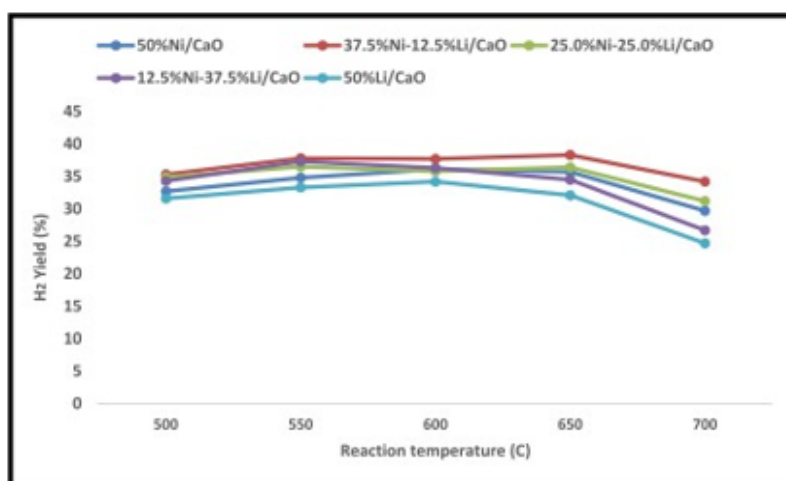


Figure 10: Effect of reaction temperature on hydrogen yield.

enhanced role of highly dispersed Pt and Ni nanoparticles over CeO₂ with the proper metal-support interaction in the catalysts. Moreover, the effect of reaction temperatures studied in the range of 650°C to 750°C indicated that the hydrogen yield increased significantly with increasing reaction temperature. The carbon yield was also found to be increased with the incremental addition of Pt in the Ni/CeO₂ catalysts and also with increasing the reaction temperatures [16].

When we consider CoO-MoO/Al₂O₃ the initial methane conversion rate is high, its rate rapidly decreases in the first half-hour and then its rate gradually decreases. The diminished methane conversion is due to the deactivation of the catalyst. The reason for catalyst deactivation is well reported, it can be attributed to the carbon deposited on the catalyst surface to cover active sites (site-blocking) or build-up at the entrance of the pores (pore-mouth plugging) [48]. It is well known that the process of carbon filaments formation is divided into three stages [49]. The first stage, the induction period, involves the decomposition of methane on the Co₃O₄ surface into carbon and hydrogen, leading to carbon deposition on the Co₃O₄ surface to form a layer of surface carbon. Thus, the initial methane conversion is high as there are plenty of active Co₃O₄ surfaces in the early stage [17].

The second step involves the lengthening of the filamentous carbon. At this stage, the surface carbon layer diffuses to the rear of the Co₃O₄ particles, and carbon is excreted to form a wall of CNTs. As a result, the active Co₃O₄ surface is covered by growing CNTs, causing a rapid decrease in methane conversion. The final stage is deactivation of the catalyst. This can be attributed to the fragmentation, encapsulation and concealment of Co₃O₄ particles by carbon. Thus, in the methane conversion profiles, it can be seen that methane conversion gradually decreases until the active sites deactivate completely [17].

Metal loading of the catalyst greatly influenced the carbon yield, diameters distribution of CNTs and the CoO-MoO crystallite sizes. An increase in the metal loading led to increasing the yield of carbon for catalysts with 10, 20 and 30 wt% loadings. It was also found that an increase in metal loading widened the diameter distributions of the as-produced CNTs. The carbon yields were found to decrease in the order 30>20>40> 10wt%. The activity of the catalysts can be related to the cobalt oxide crystallite size, in which larger sized cobalt oxide crystallite yields higher carbon deposits. In addition, CO_x-free hydrogen is produced simultaneously with CNTs from the decomposition of methane. The findings show that by increasing the metal loadings of the catalyst, one can increase the production of hydrogen by using the same amount of catalyst [17].

Sometimes molten forms of these metals are considered as catalysts. This is preferred as it prevents any carbon from being deposited on the catalyst surface, at least for a while. Thus it can help in delaying the deactivation of the catalysts. The only report of the use of a molten metal as a catalyst for CH₄ pyrolysis, described pure liquid magnesium (Mg), which was used to achieve ~30% of the equilibrium conversion at 700°C [50]. Higher conversions, at higher temperatures, were not possible because of Mg evaporation. However, in the experiment liquid alloys of active metals in low-melting temperature metal "solvents" (Sn, Pb, Bi, In, and Ga) were used with known equilibrium phase behavior to produce catalysts that melt at <1000°C, and examined the catalytic properties of such melts [18]. The melts are used in molten-metal bubble columns, where carbon continuously floats to the surface where it can be removed.

Four trends are notable. First, low-melting temperature metal "solvents" had some activity, in the order In<Bi<Sn<Ga <Pb. Second,

the addition of an active component increases the reaction rate and the magnitude of this increase depends on the solvent metal used. For example, the activity of melts containing 17 mole % of Ni increased as the solvent changed, the order being In<Sn<Ga<Pb< Bi. Third, the activity increased with the amount of the active metal, for example, 73 mole % of Ni in In was more active than 17 mole % of Ni in In. Fourth, Ni was always more active than Pt, for the same solvent, whereas solid Pt and solid Ni have approximately the same activity [51]. Of the compositions we tested, 27-mole % of Ni dissolved in molten Bi (Ni0.27Bi0.73) was the most active catalyst we found, and further experimental work focused on this alloy [18].

Finally, we come to the last but one of the most promising methods we saw outside the normal CDM methods. When non-thermal plasma was used in dry reforming with a catalyst, this enabled the reaction to occur at as low as 300°C. Use of zeolite A reduces CH₄ and CO₂ conversions but inhibits the formation of carbon black. The combination of a plasma jet with Ni/γ-Al₂O₃ increases both CH₄ and CO₂ conversion [52,53].

The experiments were performed while the plasma zone was filled with balls of glass, alumina or lanthanum oxide on alumina (La₂O₃:5 and 10 wt%). The CO₂ conversion is stabilized at about 10% with or without lanthanum. CO₂ transformation is very low at the beginning of the reaction over Al₂O₃. The presence of lanthanum oxide favours the conversion of CO₂ during the first minutes of reaction, the plateau is reached after 10 min for 10% La₂O₃/Al₂O₃, while 20 and 30 min are necessary for 5% La₂O₃/Al₂O₃ and Al₂O₃ respectively. The basic properties of lanthanum oxide could explain this behaviour. A higher amount of lanthanum oxide (10 wt%) favours methane conversion. The methane conversion is significantly higher in the presence of alumina balls compared to glass balls (21.7% against 17.5%). A significant increase in methane conversion with time on stream suggests a modification of the catalyst surface under the plasma discharge [7].

The presence of a catalyst in the plasma zone significantly increases the conversions of CO₂ and CH₄ at 300°C relative to glass balls. We have checked that experiments performed with a catalyst (without plasma discharge) at 300°C do not show any conversions of CO₂ and CH₄, proving that a positive interaction occurs between the catalyst and the plasma discharge even with bare alumina balls. This synergy effect is more pronounced in presence of lanthanum oxide, the CH₄ and CO₂ conversion reaching respectively, 47.6% and 10.0% for 10% La₂O₃/Al₂O₃ catalyst. A higher amount of lanthanum (20% La₂O₃/Al₂O₃) leads to a lower methane conversion, most probably due to the lower surface area or to the non-optimal dispersion of the active phase. The addition of lanthanum at the surface of alumina balls significantly increases methane conversion while the average CO₂ conversion is not significantly modified [7].

A synergism between a Cu-Ni/Al₂O₃ catalyst and a dielectric barrier discharge plasma was evidenced, at 450°C [54]. The conversions of CH₄ and CO₂ reached 69% and 75% respectively with a discharge power of 60W, while with plasma only, the conversions were very low (13% for CH₄ and less than 5% for CO₂). Thus we can say it's possible to find a certain midground between temperature and conversion to give us the optimum conditions necessary for this to be made commercially viable.

Conclusion

There were multiple similarities between each of the papers we

reviewed. The most common catalysts used were Nickel and Iron. These catalysts were doped with metals like copper and oxides of titanium were used to increase its effectiveness. Multiple promoters that consisted of compounds like oxides of lanthanum and tungsten were used which enhanced the properties of the catalyst.

The most common difficulties were that the catalyst deactivated after a certain period of time as the carbon produced in the reaction clogged the pores of the catalyst thus reducing its activity. The second was that most of the reactions took place above 700°C. But there were few that had a positive response at lower temperatures as well. There were ways to tackle this problem, as it was possible to make this carbon react with steam parallelly. This reaction would give hydrogen and carbon monoxide. Thus, it would produce more hydrogen than the original and also prevent the catalyst from deactivating. The carbon monoxide produced could also be further used in the water gas shift reaction ultimately giving more hydrogen.

The other products like carbon, which are produced along with Hydrogen, can be reused depending upon the purity with which it is formed. The resulting carbon occasionally forms either as nanofibers or as graphite, which can both be put to use in different industries.

After studying multiple papers about different catalysts, we concluded that the most suitable catalyst would not be a single one as it would depend on the usage of the hydrogen and carbon produced. Nickel and Iron are the best candidates with Nickel having an edge as when doped with the right metal, say copper or titanium dioxide along with a promoter, it would act at much lower temperatures and be much more stable than its iron counterpart. However, if the usage of Hydrogen would be industrial then in some cases Iron would be preferred. The choice of promoter would also most likely be oxides of either Lanthanum or Tungsten and Aluminium. Molten metal catalysts also seemed to be effective in controlling the degradation of the catalyst, however it does react at higher temperatures and needs more development in order to be industrially feasible as well.

Other methods such as using non-thermal plasma in the reforming methane were also studied. The plasma discharge was coupled with Nickel and Aluminium dioxide, which reacted at temperatures as low as 300°C. This was one of the few methods that do not completely fall under CDM that produced results that were impressive. However, conversion rates weren't high enough in order for this method to be used on a large scale basis. Using different catalysts at different reaction conditions can allow us to increase these rates as stated in the case of Cu-Ni/Al₂O₃ at 450°C, which allows us to make this method commercially viable.

Note: All images taken from papers as referenced in the text.

References

1. Abánades A, Rubbia C, Salmieri D (2013) Thermal cracking of methane into Hydrogen for a CO₂-free utilization of natural gas. *Int J Hydro Energy* 38: 8491-8496.
2. Keller M, Matsumura A, Sharma A (2020) Spray-dried Fe/Al₂O₃ as a carbon carrier for CO_x-free hydrogen production via methane cracking in a fluidized bed process. *Chem Engg J* 398: 125612.
3. Torres D, Llobet S, Pinilla JL, Lázaro MJ, Suelves I, Moliner R (2012) Hydrogen production by catalytic decomposition of methane using a Fe-based catalyst in a fluidized bed reactor. *J Nat Gas Chem* 21: 367-373.
4. Fakeeha A, Kasim S, Ibrahim AA, Al-Awadi AS, Alzahrani E, Abasaeed AE, et al. (2020) Methane decomposition over ZrO₂-supported Fe and Fe-Ni catalysts- Effects of doping La₂O₃ and WO₃. *Front Chem* 8: 317.
5. Awad A, Salam MA, Dai-Viet NV, Abdullah B (2020) Hydrogen production via thermocatalytic decomposition of methane over Ni-Cu-Pd/Al₂O₃ catalysts. *Mat Sci Eng* 736: 042006.
6. Hussein S, Zein SH, Rahman M, Sessa P, Sai T (2004) Kinetic studies on catalytic decomposition of methane to hydrogen and carbon over Ni/TiO₂. *Industr Eng Chem Res* 43: 4864-4870.
7. Yap D, Tatibouët JM, Dupeyrat CB (2017) Catalyst assisted by non-thermal plasma in dry reforming of methane at low temperature. *Catalysis Today* 299: 20.
8. Chin SY, Chin HY, Amiridis MD (2006) Hydrogen production via the catalytic cracking of ethane over Ni/SiO₂ Catalysts. *App Cat Gen* 300: 8-13.
9. Monnerat B, Kiwi-Minsker L, Renken A (2001) Hydrogen production by catalytic cracking of methane over nickel gauze under periodic reactor operation. *Chem Eng Sci* 56: 633-639.
10. Zhu W, Xia C, Fan J, Peng R, Meng G (2006) Ceria coated Ni as anodes for direct utilization of methane in low-temperature solid oxide fuel cells. 160: 897-902.
11. González O, Valenzuela M, Wang J (2005) Catalytic decomposition of methane over cerium-doped Ni Catalysts. *MRS Proceedings* 885: 49.
12. Awad A, Salam A, Abdullah B (2017) Thermocatalytic decomposition of methane/methanol mixture for hydrogen production: Effect of nickel loadings on alumina support. *AIP Conference Proceedings* 1891: 020030.
13. Fakeeha AH, Ibrahim AA, Naeem MA, Khan WU, Abasaeed AE, Alotaibi RL, et al. (2015) Methane decomposition over Fe supported catalysts for hydrogen and nano carbon yield. *Cataly Sustain Energy* 2: 71-82.
14. Ashok J, Reddy PS, Raju G, Subramanyam M, Venugopal A (2009) Catalytic decomposition of methane to hydrogen and carbon nanofibers over Ni-Cu-SiO₂ catalysts. *Energy Fuel* 23: 5-13.
15. Musamali R, Isa YM (2018) A novel catalyst system for methane decomposition. *Energy Res* 42: 4372-4382.
16. Pudukudy M, Yaakob Z, Jia Q, Takriff MS (2018) Catalytic decomposition of undiluted methane into hydrogen and carbon nanotubes over Pt promoted Ni/CeO₂ catalysts. *New J Chem* 42: 14843-14856.
17. Lee KY, Yeoh WM, Chai SP, Ichikawa S, Mohamed AR (2013) Catalytic decomposition of methane to carbon nanotubes and hydrogen: The effect of metal loading on the activity of CoO-MoO/Al₂O₃ catalyst. *Fullerenes Nanotubes Carbon Nanostruc* 21: 158-170.
18. Upham DC, Agarwal V, Khechfe A, Snodgrass ZR, Gordon MJ, Metiu H, et al. (2017) Catalytic molten metals for the direct conversion of methane to hydrogen and separable carbon. *Science* 358: 917-921.
19. https://en.wikipedia.org/wiki/Incipient_wetness_impregnation
20. Muradov NZ (1998) CO₂-free production of hydrogen by catalytic pyrolysis of hydrocarbon fuel. *Energy Fuels* 12: 41-48.
21. Anjaneyulu C, Naresh G, Kumar VV, Tardio J, Rao TV, Venugopal A (2018) Influence of rare earth (La, Pr, Nd, Gd, and Sm) metals on the methane decomposition activity of Ni-Al catalysts. *Am Chem Soc* 3: 1298-1305.
22. Chen L, Qi Z, Zhang S, Su J, Somorjai GA (2020) Catalytic hydrogen production from methane: A review on recent progress and prospect. *Catalysts* 10: 858.
23. Park S, Vohs JM, Gorte RJ (2000) Direct oxidation of hydrocarbons in a solid-oxide fuel cell. *Nature* 404: 265-267.
24. Gorte RJ, Park S, Vohs JM, Wang C (2000) Anodes for direct oxidation of dry hydrocarbons in a solid-oxide fuel cell. *Adv Mater* 12: 1465-1469.
25. Ibrahim AA, Fakeeha AH, Al-Fatesh AS, Abasaeed AE, Khan WU (2015) Methane decomposition over iron catalyst for hydrogen production. *Int J Hydro Energy* 40: 7593-7600.
26. Saraswat SK, Pant KK (2013) Synthesis of carbon nanotubes by thermo catalytic decomposition of methane over Cu and Zn promoted Ni/MCM-22 catalyst. *J Environment Chem Eng* 1: 746-754.
27. Bayat N, Rezaei M, Meshkani F (2015) Methane decomposition over Ni-Fe/Al₂O₃ catalysts for production of CO_x-free hydrogen and carbon nanofiber. *Int J Hydro Energy* 41: 53.

28. Awad A, Salam MA, Dai-Viet NV, Abdullah B (2020) Hydrogen production via thermocatalytic decomposition of methane over Ni-Cu-Pd/Al₂O₃ catalysts. *Mat Sci Eng* 736: 042006.
29. Zhang J, Xie W, Li X, Hao Q, Chen H, Ma X (2018) Methane decomposition over Ni/carbon catalysts prepared by selective gasification of coal char. *Energy Conv Manage* 177: 330-338.
30. Awadallah AE, Aboul-Enein AA, Aboul-Gheit AK (2014) Impact of group VI metals addition to Co/MgO catalyst for non-oxidative decomposition of methane into CO_x-free hydrogen and carbon nanotubes. *Fuel* 129: 27-36.
31. Yokoyama H, Numakura H, Koiwa M (1998) The solubility and diffusion of carbon in palladium. *Acta Materialia* 46: 2823-2830.
32. Baker RTK, Harris PS (1978) *Chemistry and physics of carbon*. Marcel Dekker Inc 14: 309.
33. Baker RTK (1979) In situ electron microscopy studies of catalyst particle behavior. *Cat Rev* 19: 161-209.
34. Audier M, Coulon M (1985) Kinetic and microscopic aspects of catalytic carbon growth. *Carbon* 23: 317-323.
35. Alstrup I (1988) A new model explaining carbon filament growth on nickel, iron, and Ni-Cu alloy catalysts. *J Catalysis* 109: 241-251.
36. Dresselhaus MS, Dresselhaus G, Sugihara K, Spain IL, Goldberg HA (1988) *Graphite fibers and filaments*. Springer.
37. Baker RTK (1989) Catalytic growth of carbon filaments. *Carbon* 27: 315-323.
38. Yang RT, Chen JP (1989) Mechanism of carbon filament growth on metal catalysts. *J Catalyst* 115: 52-64.
39. Ermakova MA, Ermakov DY, Kuvshinov GG, Plyasova LM (1999) New nickel catalysts for the formation of filamentous carbon in the reaction of methane decomposition. *J Catalyst* 187: 77-84.
40. Bengaard HS, Nørskov JK, Sehested J, Clausen BS, Nielsen LP, Molenbroek AM, et al. (2002) Steam Reforming and Graphite Formation on Ni Catalysts. *J Catalyst* 209: 365-384.
41. Snoeck JW, Froment GF, Fowles M (1997) Filamentous carbon formation and gasification: thermodynamics, driving force, nucleation, and steady-state growth. *J Catalyst* 169: 240-249.
42. Murray EP, Tsai T, Barnett SA (1999) A direct-methane fuel cell with a ceria-based anode. *Nature* 400: 649-651.
43. Morel B, Laurencin J, Bultel Y, Lefebvre-Joud F (2005) Anode-supported SOFC model centered on the direct internal reforming. *J Electrochem* 152: A1382-A1389.
44. Fajardie F, Tempere JF, Manolo JM, Djega-Mariadassou G, Blanchard G (1998) Ceria lattice oxygen ion substitution by Cl⁻ during the reduction of Rh(Cl)/CeO₂ catalysts. Formation and stability of CeOCl. *J Chem Soc* 94: 3727-3735.
45. Fallah JE, Boujana S, Dexpert H, Kiennemann A, Majerus J, Touret O, et al. (1994) redox processes on pure ceria and on Rh/CeO₂ catalyst monitored by X-Ray absorption (Fast Acquisition Mode). *J Phys Chem* 98: 5522-5533.
46. Li Z, Chen J, Zhang X, Li Y, Fung KK (2002) Catalytic synthesized carbon nanostructures from methane using nanocrystalline Ni. *Carbon* 40: 409-415.
47. Adams BD, Ostrom CK, Chen S, Chen A (2010) High-Performance Pd-Based hydrogen spillover catalysts for hydrogen storage. *J Phys Chem* 114: 19875-19882.
48. Ashok J, Reddy PS, Raju G, Subramanyam M, Venugopal A (2009) Catalytic decomposition of methane to hydrogen and carbon nanofibers over Ni-Cu-SiO₂ catalysts. *Energy Fuel* 23: 5-13.
49. Tavares MT, Bernardo CA, Alstrup I, Rostrup-Nielsen JR (1986) Reactivity of carbon deposited on nickel-copper alloy catalysts from the decomposition of methane. *J Catalyst* 100: 545-548.
50. Wang K, Li WS, Zhou XP (2008) Hydrogen generation by direct decomposition of hydrocarbons over molten magnesium. *J Mol Cataly* 283: 153-157.
51. Choudhary TV, Aksoylu E, Goodman DW (2003) Nonoxidative activation of methane. *Catalysis Rev* 45: 151-203.
52. Wang T, Liu H, Xiong X, Feng X (2017) Conversion of carbon dioxide to carbon monoxide by pulse dielectric barrier discharge plasma. *Earth Environment Sci* 52: 012100.
53. Pietruszka B, Heintze M (2004) Methane conversion at low temperature: The combined application of catalysis and non-equilibrium plasma. *Catalysis Today* 90: 151-158.
54. Zhang AJ, Zhu AM, Guo j, Xu Y, Shi C (2010) Conversion of greenhouse gases into syngas via combined effects of discharge activation and catalysis. *Chem Eng J* 156: 601-606.